MICRO-FTIR AND MICRO-RAMAN SPECTROSCOPY OF SHOCKED BASALTS FROM LONAR CRATER, INDIA. T. D. Glotch[1], S. P. Wright[2], B. E. McKeeby[1], and M. J. Ferrari[1], [1]Stony Brook University, 255 Earth and Space Sciences, Stony Brook, NY 11794-2100, tglotch@notes.cc.sunysb.edu, [2]University of New Mexico

Introduction: Mars, the Moon, and other planetary bodies have been subjected to intense bombardment by meteorites throughout their histories. Understanding the effects of this bombardment on the crystal structures of target materials is a first-order problem in planetary science that has important implications for planetary remote sensing and *in situ* mineralogical studies.

Lonar Crater, located in central India, represents a unique terrestrial analog for planetary impact studies in that it represents a relatively recent (~ 500 ka) impact into a basaltic crust. Within the ejecta layer are basaltic rocks shocked at intermediate pressures of 20-80 GPa [1]. Other terrestrial impact craters primarily occur in typical continental crust or sedimentary settings. The basaltic composition of the Lonar impact crater makes it the only terrestrial impact analog suitable for understanding the effects of impact on the composition of the Martian basaltic crust and lunar mare.

Several studies have detailed the mid-IR spectroscopic properties of synthetically shocked plagioclase feldspar and pyroxene-rich samples and basalts [2-4]. Recent studies have also detailed the macroscopic mid-IR spectral properties of naturally shocked basalts from Lonar Crater [1,5]. Here, we provide micro-FTIR and micro-Raman data for both shocked and unshocked basalts from Lonar Crater. These data provide a detailed view of the petrography of Lonar samples and indicate that the effects of shock are not homogenous throughout the material undergoing shock compression.

Samples and Methods: We analyzed several samples of shocked and unshocked basalt from Lonar Crater collected by S. P. Wright and described further in [6]. Three samples, LC09-206, LC09-207, and LC09-284 were selected for analysis. LC09-206 and LC09-284 are shock class 2 samples (20-40 GPa shock pressure) [7], while LC09-207 is an unshocked basalt collected in the same suevite breccia outcrop as the other two shocked basalts that displays a minor amount of weathering. Samples were cut and polished into thick sections with a roughness of 0.25 µm.

Each of the samples was examined using the Stony Brook University Vibrational Spectroscopy Laboratory's [8] Nicolet iN10MX FTIR microscope equipped with a liquid nitrogen cooled MCT array detector. This instrument is capable of acquiring hyperspectral image cubes between 7000 and 715 cm^{-1} at a spatial resolution of 25 µm/pixel.

Each sample was also studied using VSL's Wi-TEC alpha300R confocal Raman microscope system equipped with a 50 mW frequency doubled 532 nm Nd:YAG excitation laser. This Raman imaging spectrometer acquires spectra from ~8000-150 Δcm^{-1} and is equipped with multiple objective lenses enabling spatial resolutions between several microns and 260 nm/pixel.

Results and Discussion: Both LC09-206 and LC09-284 contain abundant maskelynite (feldspathic glass) formed as a result of the shock process. These samples also contained unshocked clinopyroxene and and melt glass, either in veins or pockets.

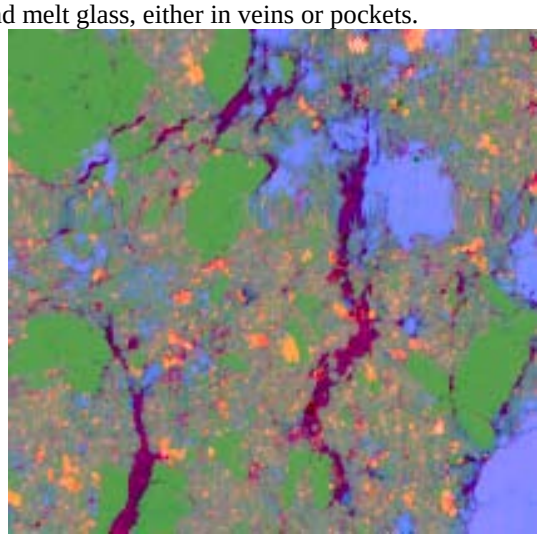

Figure 1. DCS FTIR reflectance image displaying the spectral variability in sample LC09-206. Green pixels correspond to maskelynite, blue/purple pixles correspond to melt glass, orange pixels correspond to clinopyroxene, and red/purple pixels correspond to epoxy used in the sample preparation process.

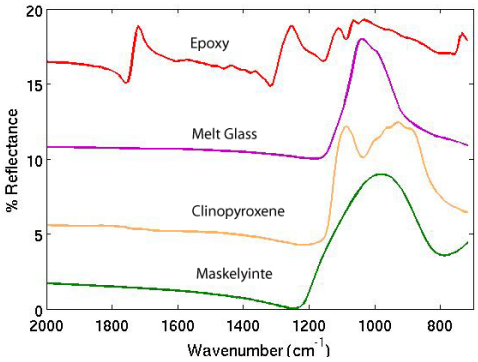

Figure 2. Representative spectra from each of the color units shown in Figure 1.

Micro-FTIR Data: We created 5 x 5 mm hyperspectral reflectance maps of sections of each of the three samples. Initial inspection of the data revealed both maskelynite and melt glass, each with a strong reflectance peak near 1000 cm^{-1}. The spectra differ primarily in the width of the main Si-O stretching band, with the maskelynite feature being significantly broader than the melt glass feature. We created simple spectral indices based on the positions of these and other common spectral features present in the map and combined them in a decorrelation-stretched (DCS) image, displaying spectral differences as color variance. The DCS image for sample LC09-206 is shown in Figure 1, and spectra corresponding to the color units displayed in the image are shown in Figure 2.

A second analysis method involves using linear deconvolution to map mineral abundances across an image using a library of spectral endmembers. To analyze sample LC09-207, we converted the reflectance map to emissivity using Kirchhoff's Law (ε = 1-R) and utilized a spectral library consisting of 150 pure mineral emissivity spectra. Results of the deconvolution are generally consistent with petrographic analysis, which shows a pyroxene- and plagioclase-dominated rock with some serpentine and calcite. Figure 3 shows a false-color map created by combining the plagioclase, clinopyroxene, and serpentine abundance maps determined by the deconvolution algorithm.

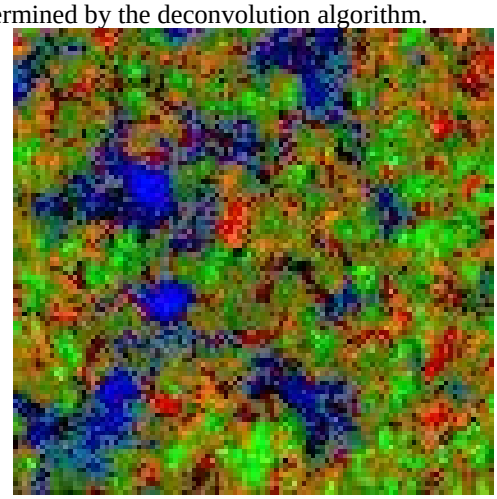

Figure 3. A false color infrared image of LC09-207 created by combining abundance images for plagioclase (red), pyroxene (green), and serpentine (blue). The image is 5 mm across.

Although linear deconvolution can be a useful method to determine the mineral distributions within a sample, it should be used with caution in this case. Complications resulting from the deconvolution of reflectance data using an emissivity spectral library are currently unquantified. Furthermore, spectral endmembers represent the sum of all possible mineral orientations for any given mineral, while at the 25 µm spatial scale, significant spectral anisotropy due to crystal orientation is to be expected. Further work is required to quantify these effects.

Micro-Raman Data: Raman data are highly complimentary to the FTIR data discussed above, but they also provide a unique perspective on the mineralogy of the shocked basalt samples. In general, it is possible to determine the mineralogy of much smaller (260 nm to a few µm) grains using the Raman system, while typical micro-FTIR reflectance data are 25 µm/pixel. Figure 4 shows background-removed labradorite and augite spectra (705 nm spot size) from the unshocked LC09-207 sample and maskelynite and melt glass spectra from the shocked LC09-206 sample. Similar to the FTIR spectra, the maskelynite and melt glass Raman spectra differ, with maskelynite displaying broad peaks between 500 and 600 Δcm^{-1} and ~900-1100 Δcm^{-1}. The melt glass spectrum displays a comparatively sharp peak centered at 590 Δcm^{-1} and a weaker, broader peak centered at 1090 Δcm^{-1}. Both spectra differ markedly from the crystalline spectra from the unshocked sample. Future work will concentrate on creating Raman maps with sub-µm spatial resolution in an effort to determine the effects of shock on potential accessory minerals and to study the effects of aquesous weathering on these samples.

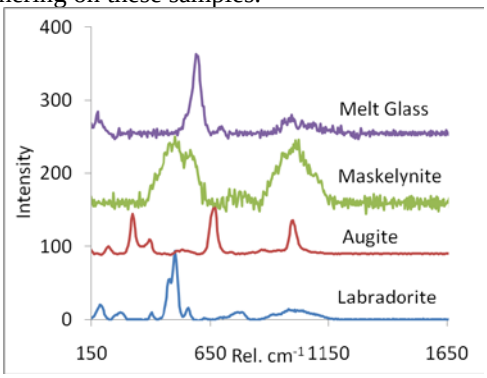

Figure 4. Micro-Raman spectra acquired from samples LC09-284 (labradorite and augite) and LC09-206 (maskelynite and melt glass). Spectra were acquired using a 532 nm excitation laser and a 20 X, 0.46 N.A. objective, leading to a 705 nm spot size.

References: [1] Wright S. P. et al. (2008) *LPS XXXIX*, Abstract 2330. [2] Johnson J. R. et al. (2002) *JGR*, 107(E10), 5073. [3] Johnson J. R. et al. (2003) *Am. Miner.*, 88, 1575-1582. [4] Johnson J. R. et al. (2007) *Am. Miner*, 92, 1148-1157. [5] Wright S. P. et al. (2011) *JGR*, in review. [6] Wright S. P. and H. E. Newsom (2011) *LPS XVII*, Abstract 1619. [7] Kieffer S. W. (1976) *LPS VII*, 1391-1412. [8] Glotch T. D. et al. (2011) *LPS XVII*, Abstract 1307.